

LFU and CP violation with S_3 Nejc Košnik^{1,2,*} and Aleks Smolkovič^{2,†}¹*Department of Physics, University of Ljubljana, Jadranska 19, 1000 Ljubljana, Slovenia*²*Jožef Stefan Institute, Jamova 39, P. O. Box 3000, 1001 Ljubljana, Slovenia*

We introduce the CP violating scalar leptoquark S_3 to explain the measured values of the lepton universality ratios $R_{K^{(*)}}$. We derive constraints on the CP-even and CP-odd components of the leptoquark Yukawa couplings stemming from effects in $b \rightarrow s\mu\mu$ and B_s mixing. For the $b \rightarrow s\mu\mu$ processes we impose $R_{K^{(*)}}$, $\mathcal{B}(B_s \rightarrow \mu^+\mu^-)$, as well as CP-sensitive angular asymmetries $A_{7,8,9}$, whereas in the B_s mixing sector ΔM_s and $S_{\psi\phi}$ are considered. Combining the constraints within the S_3 model reveals that a large CP phase with a definite sign is perfectly viable for a leptoquark of mass below a few TeV. For larger mass of the S_3 leptoquark the CP phase is suppressed due to the observables pertaining to the B_s system. We provide predictions of direct and mixing-induced CP asymmetries in $B \rightarrow K\mu\mu$ that could reveal the presence of the novel CP phase.

I. INTRODUCTION

The flavour structure of the Yukawa sector is probably the least understood aspect of the Standard Model (SM). In regard to the quark Yukawa couplings, numerous experiments have confirmed the general validity of the Cabibbo-Kobayashi-Maskawa (CKM) paradigm, which predicts all quark flavour transitions in terms of four parameters. The CKM matrix has small flavour violating elements and a unique phase that drives all CP-violating quantities. Furthermore, flavour changing neutral quark currents (FCNC) are suppressed due to only occurring at higher order in perturbation theory, as well as due to the unitarity of the CKM matrix via the Glashow-Iliopoulos-Maiani mechanism. On the contrary, in the lepton sector, the Pontecorvo-Maki-Nakagawa-Sakata mixing matrix exhibits large flavour mixing, however the smallness of neutrino masses renders this effect unobservable in experiments blind to neutrino flavours. Consequently, the flavour of charged leptons is conserved and couplings of leptons to gauge bosons are lepton flavour universal (LFU), whereas differing masses of leptons explicitly break LFU. Thus, in a LFU ratio of two processes, which are related by a lepton flavour rotation, systematic errors largely cancel, provided there is a large overlap in the phase space [1, 2].

The LFU predictions have been tested in various processes on energy scales ranging from kaon decays, weak boson decays $Z \rightarrow \ell\ell$ at LEP [3], to highest energy tests at the Large Hadron Collider (LHC) [4]. In the last decade, the LHCb experiment presented measurements of LFU-sensitive ratios $R_{K^{(*)}} \equiv \Gamma'(B \rightarrow K^{(*)}\mu\mu)/\Gamma'(B \rightarrow K^{(*)}ee)$, where Γ' stands for the partial width in the region $q^2 \in [1.1, 6] \text{ GeV}^2$, and found

$$\begin{aligned} R_K &= 0.846_{-0.039-0.012}^{+0.042+0.013} \quad [5-7], \\ R_{K^*} &= 0.69_{-0.07-0.05}^{+0.11+0.05} \quad [8]. \end{aligned} \quad (1)$$

The ratios are 3.1 and 2.6σ below their SM predictions, $R_{K^{(*)}} = 1.00(1)$ [9]. Driven by FCNC, this process is GIM suppressed, which allows potential New Physics (NP) contributions to stand out. In the effective Hamiltonian description the presence of a NP effective operator with left-handed fermions $\mathcal{O}_9 - \mathcal{O}_{10} \propto (\bar{s}_L\gamma^\mu b_L)(\bar{\mu}_L\gamma_\mu\mu_L)$ is in good agreement with measurements in Eq. (1), as well as with the global set of $b \rightarrow s\mu\mu$ observables [10, 11]. Scalar or vector leptoquarks (LQs) at the TeV scale can naturally generate such effective operators at tree-level, see e.g. [12]. The discrepancies in Eq. (1) pull the value of the NP Wilson coefficient $\delta C_9 = -\delta C_{10}$ to negative real values and possibly large CP-violating imaginary parts, which are allowed by global analyses [11]. Such NP CP-violating phases lead to enhanced direct CP-asymmetries in $B \rightarrow K^{(*)}\mu^+\mu^-$ decays [13].

Large $\text{Im}(\delta C_9)$ imprints its CP violating effects on processes connected to $b \rightarrow s\mu\mu$ via electroweak mixing. Such a connection between the $R_{K^{(*)}}$ anomalies and the B_s mixing observables has been studied in Refs. [14–16]. In Z' and LQ models δC_9 and $B_s - \bar{B}_s$ are concurrently generated, however the correlations between the two processes are quite different in the two models. The CP violating aspects of B_s mixing and their relation to δC_9 have been studied in [14] in the context of Z' models. Connection between the $R_{K^{(*)}}$ anomalies and B_s mixing frequency Δm_s has already been studied in Refs. [15, 16].

In this paper we consider the phenomenological consequences of $\text{Im}(\delta C_9)$, generated by a concrete model with a scalar LQ $S_3 = (\mathbf{3}, \mathbf{3}, 1)$, and paying particular attention to the effects in B_s mixing. This LQ naturally realises the left-handed scenario $\delta C_9 = -\delta C_{10}$ since the gauge quantum numbers allow only Yukawa couplings to fermion doublets [2]. This LQ state was also considered in attempts to address $R_{K^{(*)}}$ and $R_{D^{(*)}}$ simultaneously [17–20] as well as in broader context including dark sectors [21, 22].

In Sec. II we perform matching onto appropriate operators for δC_9 and the B_s mixing coefficient C_{bs}^{LL} where we allow for arbitrary complex Yukawa couplings of the LQ. In Sec. III we derive constraints stemming from CP

* Electronic address: nejc.kosnik@ijs.si† Electronic address: aleks.smolkovic@ijs.si

(non-)conserving observables in $b \rightarrow s\mu\mu$ and $B_s - \bar{B}_s$ mixing. Next, we show in Sec. IV to what extent the CP conserving and violating $b \rightarrow s\mu\mu$ and B_s mixing observables Δm_s and $S_{\psi\phi}$ restrict the allowed values of δC_9 . We predict possible future signatures of the leptoquark CP phase, and finally conclude in Sec. V.

II. MATCHING

II.1. Dimension-6 operators from the S_3 leptoquark

Here we present the effects of the S_3 LQ via the matching onto the left-handed four-fermion operators of the SMEFT [23–26]. We pick only those LQ Yukawa couplings at the matching scale that are necessary to induce the operators with the flavor structure $(\bar{s}b)(\bar{\mu}\mu)$.

The starting point is the Lagrangian of the S_3 leptoquark [27]

$$\mathcal{L} = |D_\mu S_3|^2 - m_{S_3}^2 |S_3|^2 + y_{ij} \bar{Q}_i^C (i\tau^2 \tau^I) L_j S_3^I, \quad (2)$$

where the index $I = 1, 2, 3$ runs over the weak isospin generators. We assume that the quark flavour index $i = d, s, b$ refers to the down-quark mass eigenstates, forcing the CKM matrix V to appear alongside up-type quark mass eigenstates, $Q_i = (V_{ki}^* u_{L,k}, d_{L,i})^T$. We have neglected neutrino masses and used the index j to refer to charged lepton mass eigenstates. Our basic assumption is that at scale m_{S_3} only the Yukawa couplings $y_{b\mu}$ and $y_{s\mu}$ are non-zero to accommodate $R_{K^{(*)}}$ measurements, and that these couplings can take complex values. We match onto the SMEFT Lagrangian, defined as $\mathcal{L}_{\text{dim-6}} = \sum_i C_i \mathcal{O}_i$, and find that the following semileptonic operators are generated at tree-level:

$$Q_{lq}^{(1)} = (\bar{L}_p \gamma^\mu L_r) (\bar{Q}_s \gamma_\mu Q_t), \quad (3)$$

$$Q_{lq}^{(3)} = (\bar{L}_p \gamma^\mu \tau^I L_r) (\bar{Q}_s \gamma_\mu \tau^I Q_t). \quad (4)$$

The flavour indices $(pqrst) = (\mu\mu sb)$ are fixed by the LQ Yukawa couplings $y_{b\mu}$ and $y_{s\mu}$ that enter the corresponding Wilson coefficients

$$C_{lq}^{(1)} = \frac{3y_{b\mu}y_{s\mu}^*}{4m_{S_3}^2}, \quad C_{lq}^{(3)} = \frac{y_{b\mu}y_{s\mu}^*}{4m_{S_3}^2}, \quad (5)$$

On the other hand, at one-loop level we get four-quark operators $Q_{qq}^{(1,3)}$

$$Q_{qq}^{(1)} = (\bar{Q}_p \gamma^\mu Q_r) (\bar{Q}_s \gamma_\mu Q_t), \quad (6)$$

$$Q_{qq}^{(3)} = (\bar{Q}_p \gamma^\mu \tau^I Q_r) (\bar{Q}_s \gamma_\mu \tau^I Q_t). \quad (7)$$

with indices $(pqrst) = (sbsb)$, thus contributing at low scales to $B_s - \bar{B}_s$ mixing. The respective Wilson coefficients read

$$C_{qq}^{(1)} = -\frac{9(y_{b\mu}y_{s\mu}^*)^2}{256\pi^2 m_{S_3}^2}, \quad C_{qq}^{(3)} = -\frac{(y_{b\mu}y_{s\mu}^*)^2}{256\pi^2 m_{S_3}^2}. \quad (8)$$

Our matching results agree with Ref. [28].

II.2. From SMEFT to WET

The semileptonic operators $Q_{lq}^{(1,3)}$ at the matching scale naturally match onto the weak effective theory in the broken phase of the electroweak symmetry. Low-energy effects in $b \rightarrow s\mu^+\mu^-$ are parameterized by the following operators

$$\mathcal{H}_{\text{eff}}^{b \rightarrow s\ell\ell} = -\frac{4G_F V_{tb} V_{ts}^*}{\sqrt{2}} \sum_{i=7,9,10} C_i(\mu) \mathcal{O}_i(\mu) \quad (9)$$

and we set the scale to $\mu = m_b$. Relevant modification of the effective Wilson coefficients values in the SM [29, 30] are $C_{9,10} = C_{9,10}^{\text{SM}} \pm \delta C_9$. Note that due to the LQ flavour structure, only operators with muons are modified. The relevant operators are

$$\mathcal{O}_7 = \frac{em_b}{4\pi} (\bar{s}_R \sigma_{\mu\nu} b_R) F^{\mu\nu}, \quad (10)$$

$$\mathcal{O}_{9(10)} = \frac{e^2}{(4\pi)^2} (\bar{s}_L \gamma_\nu b_L) (\bar{\mu} \gamma^\nu (\gamma^5) \mu). \quad (11)$$

The QCD and QED renormalization group running below the weak scale of such quark current operators is negligible [31]. Thus we can read off the semileptonic coefficients at scale $\mu = m_b$ from the expressions in Eq. (5):

$$\delta C_9 = -\delta C_{10} = \frac{\pi y_{b\mu} y_{s\mu}^*}{\sqrt{2} G_F V_{tb} V_{ts}^* \alpha_{\text{em}} m_{S_3}^2}. \quad (12)$$

At loop level also the coefficient of the dipole operator gets modified by δC_7 , however the contribution is strongly suppressed by a loop factor and α , i.e. $\delta C_7 = \alpha/(8\pi) \delta C_9$.

The coefficients of the four-quark operators (8), on the other hand, match onto the $\Delta B = \Delta S = 2$ effective Lagrangian with exclusively left-handed quarks [16]

$$\mathcal{L}_{bs} = -\frac{4G_F}{\sqrt{2}} (V_{tb} V_{ts}^*)^2 C_{bs}^{LL}(\mu) (\bar{s}_L \gamma^\mu b_L)^2, \quad (13)$$

with the modification of the Wilson coefficient $C_{bs}^{LL} = C_{bs}^{LL(\text{SM})} + \delta C_{bs}^{LL}$. The SM part reads [16, 32]

$$C_{bs}^{LL(\text{SM})}(m_b) = \hat{\eta}_B \frac{m_W^2 S_0(\bar{m}_t^2/m_W^2)}{16\pi^2 v^2} \quad (14)$$

$$= (1.310 \pm 0.010) \times 10^{-3},$$

and contains the μ -dependent QCD renormalization group factor $\hat{\eta}_B = 0.84$ [32, 33] due to running to the $\mu = m_b$ scale. For the LQ contribution we match and run the coefficients $C_{qq}^{(1,3)}$ in Eq. (8) to

$$\delta C_{bs}^{LL}(\mu = m_b) = \eta^{6/23} \frac{5(y_{b\mu} y_{s\mu}^*)^2}{256\sqrt{2}\pi^2 m_{S_3}^2 G_F (V_{tb} V_{ts}^*)^2}, \quad (15)$$

where $\eta = \alpha_s(m_{S_3})/\alpha_s(m_b)$ at leading order, neglecting the top quark threshold effect [15, 33].

III. CP-EVEN AND ODD CONSTRAINTS

In this Section we present the relevant observables and derive constraints on low energy effective interactions (9) and (13).

III.1. $b \rightarrow s\mu\mu$ constraints

In order to predict $R_{K^{(*)}}$, we employ the numerical formulae

$$\begin{aligned} R_K &= 1.003 + 0.477 \operatorname{Re}(\delta C_9) \\ &\quad + 4.01 \times 10^{-3} \operatorname{Im}(\delta C_9) + 0.057 |\delta C_9|^2, \\ R_{K^*} &= 0.997 + 0.472 \operatorname{Re}(\delta C_9) \\ &\quad + 1.65 \times 10^{-3} \operatorname{Im}(\delta C_9) + 0.066 |\delta C_9|^2, \end{aligned} \quad (16)$$

valid in the region $q^2 \in [1.1, 6] \text{ GeV}^2$, as presented in Ref. [13]. The branching ratio of the B_s muonic decay has been re-measured recently by LHCb [34] and was combined with ATLAS [35] and CMS [36] in the world average that reads $\mathcal{B}(B_s \rightarrow \mu\mu) = (2.85^{+0.34}_{-0.31}) \times 10^{-9}$ [37]. The theoretical expression reads

$$\begin{aligned} \mathcal{B}(B_s \rightarrow \mu^+ \mu^-) &= \frac{\tau_{B_s}}{1 - y_s} \frac{\alpha^2 G_F^2 m_{B_s}}{16\pi^3} |V_{tb} V_{ts}^*|^2 m_\mu^2 \\ &\quad \times \sqrt{1 - \frac{4m_\mu^2}{m_{B_s}^2}} |C_{10}|^2 f_{B_s}^2, \end{aligned} \quad (17)$$

where $f_{B_s} = (230.3 \pm 1.3) \text{ MeV}$ [38], and one must also account for the effect of B_s oscillations in the time-integrated measurement of the branching fraction [39]. In Ref. [40] the authors computed power-enhanced QED corrections to the rate and found for the SM prediction $\mathcal{B}(B_s \rightarrow \mu^+ \mu^-)^{\text{SM}} = (3.66 \pm 0.14) \times 10^{-9}$. In our analysis we rescale this SM prediction as $\mathcal{B}(B_s \rightarrow \mu^+ \mu^-)^{\text{th}} = |1 + \delta C_{10}/C_{10}^{\text{SM}}|^2 \mathcal{B}(B_s \rightarrow \mu^+ \mu^-)^{\text{SM}}$, where we take for the SM value of the axial current coefficient $C_{10}^{\text{SM}} = -4.103$.

As we allow for complex Wilson coefficients $\delta C_9 \in \mathbb{C}$, we also consider the T_N -odd¹ CP-odd observables $A_{7,8,9}$, which are sensitive to CP-violating weak phases even in absence of strong phases [41]. We use the latest LHCb measurements of $A_{7,8,9}$ in $q^2 \in [1.1, 6] \text{ GeV}^2$, provided in Ref. [42]. As for the theoretical predictions, we rely on the `flavio` package [43] and check that the constraints agree with the ones provided in Ref. [11].

III.2. $B_s - \bar{B}_s$ mixing constraints

Possible contributions of NP to C_{bs}^{LL} in Eq.(13) will be susceptible to constraints from $B_s - \bar{B}_s$ mixing. The

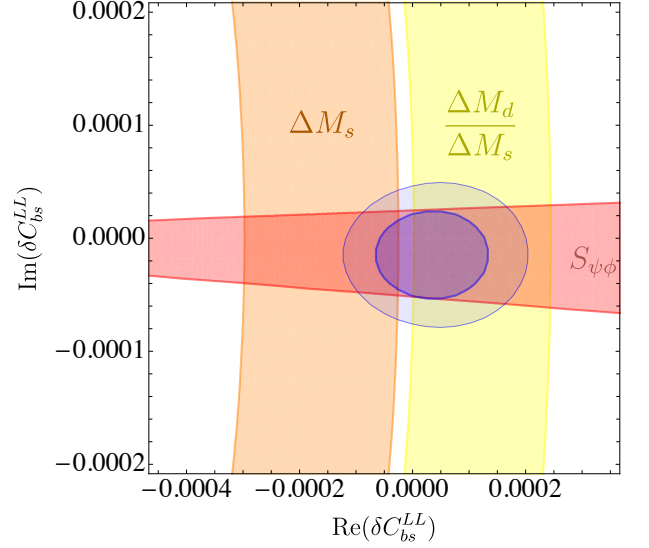


Figure 1. The 1σ constraints on δC_{bs}^{LL} due to $B_s - \bar{B}_s$ mixing observables. The dark and light blue oval regions show the 1 and 2σ fitted regions, respectively.

impact on the mass difference ΔM_s can be parametrized as

$$\Delta M_s^{\text{SM}+\text{NP}} = \Delta M_s^{\text{SM}} \left| 1 + \frac{\delta C_{bs}^{LL}(m_b)}{C_{bs}^{LL(\text{SM})}(m_b)} \right|, \quad (18)$$

where

$$\Delta M_s^{\text{SM}} = \frac{4\sqrt{2}}{3} G_F m_{B_s} C_{bs}^{LL(\text{SM})} |V_{tb} V_{ts}^*|^2 (f_{B_s} \sqrt{B_{B_s}})^2, \quad (19)$$

where $C_{bs}^{LL(\text{SM})}$ is given by Eq. (14). For the combination of the nonperturbative parameters entering the hadronic mixing amplitude we take the world average of lattice computations, $f_{B_s} \sqrt{B_{B_s}} = 0.274(8) \text{ GeV}$, prepared by the FLAG group [38]. To translate to scale-dependent B_{B_s} we use the relation $\hat{B}_{B_s}/B_{B_s}(\mu_b) = 1.519$ [16]. The CKM elements entering the SM prediction are taken from the CKMfitter tree-level fit of Summer '18 [44]², $V_{td} V_{ts}^* = -0.0424^{+0.0015}_{-0.0004}$. Using these inputs we find

$$\Delta M_s^{\text{SM}} = (20.9^{+1.4}_{-1.7}) \text{ ps}^{-1}, \quad (20)$$

which is somewhat above the world experimental average $\Delta M_s^{\text{HFLAV}} = (17.74 \pm 0.02) \text{ ps}^{-1}$ [46]. On the other hand, if we consider the ratio $\Delta M_d/\Delta M_s$, where ΔM_d is the mixing frequency of the $B_d - \bar{B}_d$ system, the theoretical

¹ The naive time reversal T_N reverses the momenta and spins of particles, not to be confused with T , which additionally exchanges the initial and final states.

² The results do not change significantly if we use NP fit of CKM parameters [45].

systematic errors are different. In our model $\Delta M_d = \Delta M_d^{\text{SM}}$ and thus the prediction reads

$$\left(\frac{\Delta M_d}{\Delta M_s}\right) = \left(\frac{\Delta M_d}{\Delta M_s}\right)^{\text{SM}} \left| 1 + \frac{\delta C_{bs}^{LL}(m_b)}{C_{bs}^{LL(\text{SM})}(m_b)} \right|^{-1}, \quad (21)$$

where the SM value now depends on the nonperturbative parameter $\xi = \frac{f_{B_s} \sqrt{B_{B_s}}}{f_{B_d} \sqrt{B_{B_d}}} = 1.206(17)$ [38] and the combination $|V_{td}/V_{ts}| = 0.215(5)$ obtained from the CKMfitter tree-level fit [44]:

$$\left(\frac{\Delta M_d}{\Delta M_s}\right)^{\text{SM}} = \frac{1}{\xi^2} \left| \frac{V_{td}}{V_{ts}} \right|^2 \frac{M_{B_d}}{M_{B_s}} = 0.0311^{+0.0018}_{-0.0017}, \quad (22)$$

which is slightly above the world average $(\Delta M_d/\Delta M_s)^{\text{HFLAV}} = 0.02855 \pm 0.00011$ [46] and suggests a positive contribution of NP to ΔM_s , contrary to what we would conclude from the ΔM_s observable alone. To overcome this quite ambiguous situation we take both observables into account to derive constraints on complex δC_{bs}^{LL} . We plot the two constraints in the complex plane of δC_{bs}^{LL} in Fig. 1 and observe that they are insensitive to $\text{Im}(\delta C_{bs}^{LL})$.

In addition, the CP asymmetry $S_{\psi\phi}$ from the interference between B_s mixing and the decay $B_s \rightarrow J/\psi\phi$ [32] can be used to constrain the CP-violating $\text{Im}(\delta C_{bs}^{LL})$. The impact of NP can be parametrized as

$$S_{\psi\phi} \equiv \sin(-2\beta_s + \delta\phi), \quad (23)$$

with

$$\delta\phi = \text{Arg} \left(1 + \frac{\delta C_{bs}^{LL}(m_b)}{C_{bs}^{LL(\text{SM})}(m_b)} \right). \quad (24)$$

We use the latest HFLAV experimental result of $S_{\psi\phi} = -0.050 \pm 0.019$ [46] in our analysis and the SM value $\beta_s = 0.0198^{+0.0012}_{-0.0009}$, again determined from the tree-level fit of CKMfitter. Fig. 1 shows constraints in the δC_{bs}^{LL} complex plane from the aforementioned B_s mixing observables, where the $S_{\psi\phi}$ cuts away significant part of the parameter space with large $\text{Im}(\delta C_{bs}^{LL})$. The combined fit to all three $B_s - \bar{B}_s$ observables is shown in blue. We will employ this region in the next Section where we will interpret these constraints in the S_3 LQ model.

IV. IMPLICATIONS FOR THE S_3 MODEL

In the context of the S_3 LQ model the $b \rightarrow s\mu\mu$ and $B_s - \bar{B}_s$ processes, considered in the preceding Section, are in one-to-one correspondence as they are determined by the same couplings. The relation between the two effective interactions that is central to our analysis is the following:

$$\delta C_{bs}^{LL} = \eta^{6/23} \frac{5G_F \alpha_{\text{em}}^2}{128\sqrt{2}\pi^4} (\delta C_9)^2 m_{S_3}^2. \quad (25)$$

Here δC_9 is given in Eq. (12). For fixed δC_9 the effect in $B_s - \bar{B}_s$ is increasingly pronounced for larger m_{S_3} . Another surprising feature is that $\delta C_9 \in \mathbb{R}$ will always increase ΔM_s , while $\Delta M_s < \Delta M_s^{\text{SM}}$ can only be attained by nonzero $\text{Im}(\delta C_9)$ (See also Ref. [16]). The CPV constraint $S_{\psi\phi}$ is not sensitive directly to CPV component $\text{Im}(\delta C_9)$ but rather to the cross term $\text{Re}(\delta C_9) \text{Im}(\delta C_9)$ between CP-conserving and CP-violating LQ couplings entering $R_{K(*)}$.

IV.1. Combined constraints

We now combine the $b \rightarrow s\mu\mu$ and B_s mixing constraints, discussed in the previous Section, in the complex δC_9 plane shown in Fig. 2. The bounds from R_K , R_{K^*} , $\mathcal{B}(B_s \rightarrow \mu\mu)$ and $A_{7,8,9}$ are all independent of m_{S_3} (at the expense of varying LQ Yukawa couplings). It is worth emphasizing that the bound from $A_{7,8,9}$ has a preferred direction in $\text{Im}(\delta C_9)$. As expected, the bounds from B_s mixing constraints are more stringent for higher S_3 masses. We show the constraints from the combined fit (Fig. 1), translated via Eq. (25), in black contours for $m_{S_3} \in \{5, 10, 15, 30\}$ TeV. The combined fit of all the considered constraints is shown in blue contours, again for the same considered masses of S_3 . With blue stars we denote benchmark points, which are defined so as to attain maximal value of $\text{Im}(\delta C_9)$ at 1σ (for given m_{S_3}).

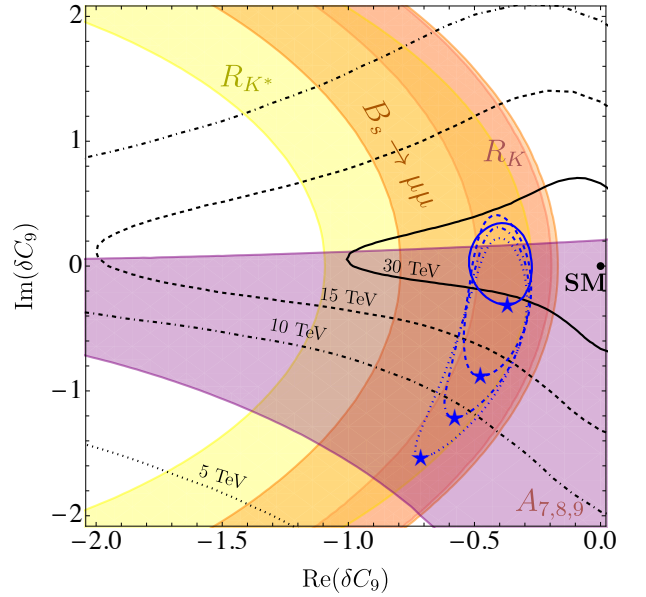


Figure 2. 1σ constraints on the δC_9 complex plane: model independent constraints from $R_{K(*)}$, $\mathcal{B}(B_s \rightarrow \mu\mu)$ and CP-odd angular coefficients $A_{7,8,9}$ from $B \rightarrow K^* \mu\mu$, as well as model dependent constraints from B_s mixing for 4 benchmark values of m_{S_3} , written on the black contours. The blue contours denote the best fit regions, with the stars showing the points of maximal allowed $\text{Im}(\delta C_9)$ for each benchmark.

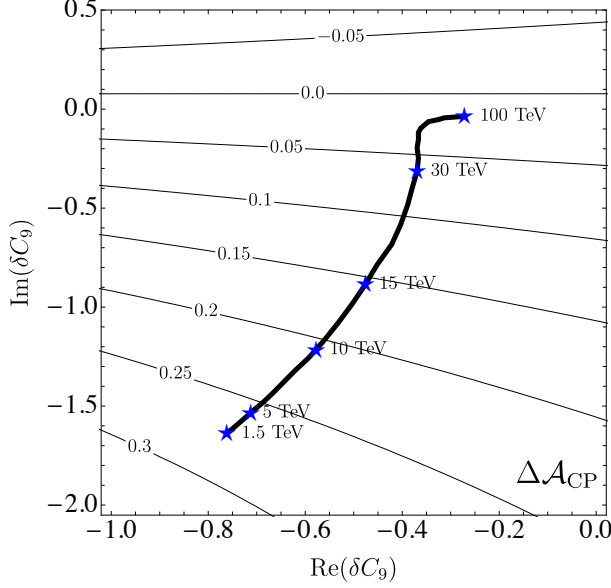


Figure 3. The predictions of the resonantly enhanced CP asymmetry in $B \rightarrow K\mu\mu$ (Eq. (27)) throughout the complex δC_9 plane. The black line shows the positions of the benchmark points from the combined fit (see Fig. 2) for m_{S_3} between 1.5 TeV and 100 TeV, with blue stars denoting some of the concrete values of m_{S_3} .

IV.2. Predictions of CPV observables

In Ref. [13] it was proposed that direct CP asymmetries \mathcal{A}_{CP} in $B \rightarrow K\mu\mu$ are enhanced due to the inter-

ference effects with narrow charmonium resonances. It was observed that one bin just below ($q^2 \in [8, 9]$ GeV²) and another just above ($q^2 \in [10, 11]$ GeV²) the J/ψ resonance, which have not been previously considered as signal region in experimental measurements [47], offer a significantly enhanced sensitivity to CP violating NP entering $b \rightarrow s\mu\mu$. The CP asymmetries $\mathcal{A}_{\text{CP}}^{[8,9]}$ and $\mathcal{A}_{\text{CP}}^{[10,11]}$ around the J/ψ peak are defined as

$$\mathcal{A}_{\text{CP}}^{[q_{\min}^2, q_{\max}^2]} \equiv \frac{\bar{\Gamma}_{[q_{\min}^2, q_{\max}^2]} - \Gamma_{[q_{\min}^2, q_{\max}^2]}}{\bar{\Gamma}_{[q_{\min}^2, q_{\max}^2]} + \Gamma_{[q_{\min}^2, q_{\max}^2]}}, \quad (26)$$

where $\bar{\Gamma}_{[q_{\min}^2, q_{\max}^2]}$ ($\Gamma_{[q_{\min}^2, q_{\max}^2]}$) denotes the partial width of the decay $\bar{B} \rightarrow \bar{K}\mu^+\mu^-$ (or its CP-conjugated mode), integrated in the kinematical region $q_{\min}^2 < q^2 < q_{\max}^2$. We do not write the units GeV in the sub- and super-scripts so as not to clutter the notation. As noted in [13] the two CP-asymmetries have opposite sign since they are separated by the J/ψ peak, suggesting that we should subtract them in order to further enhance sensitivity to $\text{Im}(\delta C_9)$:

$$\Delta\mathcal{A}_{\text{CP}} \equiv \frac{\bar{\Gamma}_{[8,9]} - \Gamma_{[8,9]} - \bar{\Gamma}_{[10,11]} + \Gamma_{[10,11]}}{\bar{\Gamma}_{[8,9]} + \Gamma_{[8,9]} + \bar{\Gamma}_{[10,11]} + \Gamma_{[10,11]}}. \quad (27)$$

We give simplified numerical formulae in terms of δC_9 for the above-defined CP asymmetries, where we assume a negative strong phase $\delta_{J/\psi}$ (see Refs. [13, 48])³:

$$\mathcal{A}_{\text{CP}}^{[8,9]} = \frac{0.0119(3) - 0.153(4) \text{Im}(\delta C_9)}{1 + 0.407(5) \text{Re}(\delta C_9) - 0.0084(2) \text{Im}(\delta C_9) + 0.055(2) |\delta C_9|^2}, \quad (28)$$

$$\mathcal{A}_{\text{CP}}^{[10,11]} = \frac{-0.0097(4) + 0.125(5) \text{Im}(\delta C_9)}{1 + 0.414(5) \text{Re}(\delta C_9) - 0.0081(3) \text{Im}(\delta C_9) + 0.053(2) |\delta C_9|^2}, \quad (29)$$

$$\Delta\mathcal{A}_{\text{CP}} = \frac{0.0108(2) - 0.139(3) \text{Im}(\delta C_9)}{1 + 0.414(5) \text{Re}(\delta C_9) - 0.0082(1) \text{Im}(\delta C_9) + 0.054(1) |\delta C_9|^2}. \quad (30)$$

The errors in the coefficients are determined by the propagation of uncertainties of the resonant parameters that enter the amplitude [13, 48]. In Fig. 3 we show the predictions of $\Delta\mathcal{A}_{\text{CP}}$ in the δC_9 complex plane with black contours. Additionally, we show with the bold black line the position of the best fit points with maximal $\text{Im}(\delta C_9)$ from considering the combined constraints on Fig. 2 for m_{S_3} between 1.5 TeV and 100 TeV. It is worth not-

ing that the perturbativity constraint on the LQ Yukawa couplings only starts playing a role at $m_{S_3} \gtrsim 200$ TeV.

Furthermore, we consider the observables sensitive to NP scenarios with CPV phases from flavour-tagged angular analysis of $B_d \rightarrow K_S \ell \ell$, proposed in Ref. [49], namely σ_0 and σ_2 . For definitions we refer the reader to Ref. [49], and instead provide a simplified formula for the $\delta C_9 = -\delta C_{10}$ scenario as

$\mathcal{A}_{7,8,9}$ in Fig. 2.

³ The choice of the $\delta_{J/\psi} < 0$ solution of the fit in Ref. [48] implies predicted \mathcal{A}_{CP} , compatible with the preferred direction from

$$\sigma_0 = \frac{0.37 - 0.02 (\text{Im}(\delta C_9))^2 + \text{Im}(\delta C_9) (-0.04 \text{Re}(\delta C_9) - 0.17) + 0.02 (\text{Re}(\delta C_9))^2 + 0.19 \text{Re}(\delta C_9)}{1 + 0.51 \text{Re}(\delta C_9) + 0.06 |\delta C_9|^2}, \quad (31)$$

whereas $\sigma_2 \approx -\sigma_0$. We provide the SM prediction, as well as some of the benchmark predictions at various masses m_{S_3} of the observable σ_0 as: $\sigma_0 = \{0.51, 0.49, 0.42, 0.38, 0.37\}$ for $\{1.5 \text{ TeV}, 15 \text{ TeV}, 30 \text{ TeV}, 100 \text{ TeV}, \text{SM}\}$, respectively. The predictions are conservative, as the uncertainties associated with hadronic effects are smaller than the last provided significant digit (Cf. [49] for a detailed discussion).

V. CONCLUSION

The persistent hints of LFU violation in $b \rightarrow s\ell\ell$ may imply an existence of leptoquarks close to the TeV scale that couple to $b\mu$ and $s\mu$. These leptoquark Yukawa couplings, necessary for the explanation of $R_{K^{(*)}}$, can in full generality be complex and thus provide a new source of CP violation.

In this paper we have considered a scalar weak-triplet leptoquark S_3 whose left-handed couplings imply the favourable $\delta C_9 = -\delta C_{10}$ scenario. We have shown that large CP violating S_3 couplings are bounded neither by $R_{K^{(*)}}$ nor by $\mathcal{B}(B_s \rightarrow \mu\mu)$, whereas existing measurements of CP asymmetries $A_{7,8,9}$ constrain $\text{Im}(\delta C_9)$, preferably towards negative values. We have considered additional signatures of the leptoquark in the B_s mixing frequency, as well as in the mixing induced CP asymme-

try $S_{\psi\phi}$. We have observed that CP-odd effects of the leptoquark in $b \rightarrow s\mu\mu$ do not necessarily entail CPV in B_s mixing. For light S_3 the B_s mixing does not play an important role, whereas for masses above 5 TeV it significantly constraints the imaginary part of δC_9 . For each mass m_{S_3} we have determined the maximal allowed CPV coupling $\text{Im}(\delta C_9)$ and derived corresponding predictions. We have pointed out potential measurements which could help pinpoint CPV in $b \rightarrow s\ell\ell$ in the future: enhanced CP asymmetries in $B \rightarrow K\mu\mu$ in the vicinity of the J/ψ resonance [13], and flavour-tagged measurements of $B_d \rightarrow K_S\ell\ell$ [49]. Such measurements, as well as increased theoretical precision in the B_s mixing observables, could help determine whether the hints of LFU violation also hint at new sources of CP violation in the Universe.

ACKNOWLEDGMENTS

The project was in part financially supported by the Slovenian Research Agency (research core funding No. P1-0035). This article is based upon work from COST Action CA16201 PARTICLEFACE supported by COST (European Cooperation in Science and Technology). A. S. is supported by the Young Researchers Programme of the Slovenian Research Agency under the grant No. 50510, core funding grant P1-0035.

-
- [1] G. Hiller and F. Kruger, Phys. Rev. D **69**, 074020 (2004), hep-ph/0310219.
 - [2] G. Hiller and M. Schmaltz, Phys. Rev. D **90**, 054014 (2014), 1408.1627.
 - [3] S. Bifani, S. Descotes-Genon, A. Romero Vidal, and M.-H. Schune, J. Phys. G **46**, 023001 (2019), 1809.06229.
 - [4] A. M. Sirunyan et al. (CMS), JHEP **07**, 208 (2021), 2103.02708.
 - [5] R. Aaij et al. (LHCb), Phys. Rev. Lett. **113**, 151601 (2014), 1406.6482.
 - [6] R. Aaij et al. (LHCb), Phys. Rev. Lett. **122**, 191801 (2019), 1903.09252.
 - [7] D. Lancierini (2021), 2105.10303.
 - [8] R. Aaij et al. (LHCb), JHEP **08**, 055 (2017), 1705.05802.
 - [9] M. Bordone, G. Isidori, and A. Pattori, Eur. Phys. J. C **76**, 440 (2016), 1605.07633.
 - [10] T. Hurth, F. Mahmoudi, D. M. Santos, and S. Neshatpour (2021), 2104.10058.
 - [11] W. Altmannshofer and P. Stangl (2021), 2103.13370.
 - [12] A. Angelescu, D. Bećirević, D. A. Faroughy, F. Jaffredo, and O. Sumensari (2021), 2103.12504.
 - [13] D. Bećirević, S. Fajfer, N. Košnik, and A. Smolkovič, Eur. Phys. J. C **80**, 940 (2020), 2008.09064.
 - [14] A. K. Alok, B. Bhattacharya, D. Kumar, J. Kumar, D. London, and S. U. Sankar, Phys. Rev. D **96**, 015034 (2017), 1703.09247.
 - [15] L. Di Luzio, M. Kirk, and A. Lenz, Phys. Rev. D **97**, 095035 (2018), 1712.06572.
 - [16] L. Di Luzio, M. Kirk, A. Lenz, and T. Rauh, JHEP **12**, 009 (2019), 1909.11087.
 - [17] A. Crivellin, D. Müller, and T. Ota, JHEP **09**, 040 (2017), 1703.09226.
 - [18] D. Bećirević, I. Doršner, S. Fajfer, N. Košnik, D. A. Faroughy, and O. Sumensari, Phys. Rev. D **98**, 055003 (2018), 1806.05689.
 - [19] V. Gherardi, D. Marzocca, and E. Venturini, JHEP **01**, 138 (2021), 2008.09548.
 - [20] A. Angelescu, D. Bećirević, D. A. Faroughy, F. Jaffredo, and O. Sumensari (2021), 2103.12504.
 - [21] S.-M. Choi, Y.-J. Kang, H. M. Lee, and T.-G. Ro, JHEP **10**, 104 (2018), 1807.06547.
 - [22] F. D'Eramo, N. Košnik, F. Pobbe, A. Smolkovič, and O. Sumensari, Phys. Rev. D **104**, 015035 (2021), 2012.05743.
 - [23] B. Grzadkowski, M. Iskrzynski, M. Misiak, and J. Rosiek, JHEP **10**, 085 (2010), 1008.4884.

- [24] E. E. Jenkins, A. V. Manohar, and M. Trott, JHEP **10**, 087 (2013), 1308.2627.
- [25] E. E. Jenkins, A. V. Manohar, and M. Trott, JHEP **01**, 035 (2014), 1310.4838.
- [26] R. Alonso, E. E. Jenkins, A. V. Manohar, and M. Trott, JHEP **04**, 159 (2014), 1312.2014.
- [27] I. Doršner, S. Fajfer, A. Greljo, J. F. Kamenik, and N. Košnik, Phys. Rept. **641**, 1 (2016), 1603.04993.
- [28] V. Gherardi, D. Marzocca, and E. Venturini, JHEP **07**, 225 (2020), [Erratum: JHEP 01, 006 (2021)], 2003.12525.
- [29] A. J. Buras, M. Misiak, M. Munz, and S. Pokorski, Nucl. Phys. B **424**, 374 (1994), hep-ph/9311345.
- [30] W. Altmannshofer, P. Ball, A. Bharucha, A. J. Buras, D. M. Straub, and M. Wick, JHEP **01**, 019 (2009), 0811.1214.
- [31] M. González-Alonso, J. Martin Camalich, and K. Mimiouni, Phys. Lett. B **772**, 777 (2017), 1706.00410.
- [32] M. Artuso, G. Borissov, and A. Lenz, Rev. Mod. Phys. **88**, 045002 (2016), [Addendum: Rev.Mod.Phys. 91, 049901 (2019)], 1511.09466.
- [33] A. J. Buras, M. Jamin, and P. H. Weisz, Nucl. Phys. B **347**, 491 (1990).
- [34] R. Aaij et al. (LHCb) (2021), 2108.09283.
- [35] M. Aaboud et al. (ATLAS), JHEP **04**, 098 (2019), 1812.03017.
- [36] A. M. Sirunyan et al. (CMS), JHEP **04**, 188 (2020), 1910.12127.
- [37] M. Algüero, B. Capdevila, S. Descotes-Genon, J. Matias, and M. Novoa-Brunet, in *55th Rencontres de Moriond on QCD and High Energy Interactions* (2021), 2104.08921.
- [38] S. Aoki et al. (Flavour Lattice Averaging Group), Eur. Phys. J. C **80**, 113 (2020), 1902.08191.
- [39] K. De Bruyn, R. Fleischer, R. Kneijens, P. Koppenburg, M. Merk, and N. Tuning, Phys. Rev. D **86**, 014027 (2012), 1204.1735.
- [40] M. Beneke, C. Bobeth, and R. Szafron, JHEP **10**, 232 (2019), 1908.07011.
- [41] C. Bobeth, G. Hiller, and G. Piranishvili, JHEP **07**, 106 (2008), 0805.2525.
- [42] R. Aaij et al. (LHCb), JHEP **02**, 104 (2016), 1512.04442.
- [43] D. M. Straub (2018), 1810.08132.
- [44] J. Charles, A. Hocker, H. Lacker, S. Laplace, F. R. Le Diberder, J. Malcles, J. Ocariz, M. Pivk, and L. Roos (CKMfitter Group), Eur. Phys. J. C **41**, 1 (2005), hep-ph/0406184.
- [45] J. Charles, S. Descotes-Genon, Z. Ligeti, S. Monteil, M. Papucci, K. Trabelsi, and L. Vale Silva, Phys. Rev. D **102**, 056023 (2020), 2006.04824.
- [46] Y. S. Amhis et al. (HFLAV), Eur. Phys. J. C **81**, 226 (2021), 1909.12524.
- [47] R. Aaij et al. (LHCb), JHEP **09**, 177 (2014), 1408.0978.
- [48] R. Aaij et al. (LHCb), Eur. Phys. J. C **77**, 161 (2017), 1612.06764.
- [49] S. Descotes-Genon, M. Novoa-Brunet, and K. K. Vos, JHEP **02**, 129 (2021), 2008.08000.